Physica **82A** (1976) 389–416 © *North-Holland Publishing Co.*

THREE-MAGNON BOUND STATES IN THE TWO-DIMENSIONAL ISOTROPIC AND ANISOTROPIC HEISENBERG FERROMAGNET

J.E. VAN HIMBERGEN and J.A. TJON

Institute for Theoretical Physics,
De Uithof, Utrecht, The Netherlands

Received 30 July 1975

The existence is shown of bound complexes of three magnons in a two-dimensional simple cubic Heisenberg ferromagnet. The Heisenberg spin hamiltonian is replaced by Dyson's boson hamiltonian. The spurious features of this hamiltonian are treated explicitly. Using Faddeev's formalism, detailed calculations of the three-magnon bound state energy curves have been performed both for the isotropic and the longitudinally anisotropic ferromagnet. Attention is paid to the possibility of observing these three-magnon bound states experimentally.

1. Introduction

Some years ago bound complexes of excitations have been observed in a one-dimensional magnetic system[1,2]). In view of this it is interesting to study the possibility of their occurrence in higher dimensional systems. For these systems it is more difficult in general to support bound states as has already been pointed out by Dyson[3]). The existence of two-magnon bound states in two- and three-dimensional Heisenberg ferromagnets has extensively been treated by Wortis[4]) and Hanus[5]). On the other hand nothing is known about the case of more than two magnons except in one dimension. There is Bethe's complete solution for the isotropic case[6]), Gochev's solution of the longitudinally anisotropic case[7]), the onset of treating the three-magnon bound state problem by means of Faddeev's formalism by Majumdar[8,9]) and a perturbation scheme to treat the two- and three-magnon problem including transverse anisotropy by Fogedby[10]).

In this paper we present results showing that in two-dimensional systems, a large variety of which are available these days[11]), bound states of three magnons exist. The most promising technique to observe bound states, that of analyzing the far infrared absorption spectra of such systems, only detects excitations that have a total momentum of approximately zero[2]). In the isotropic ferromagnet, however, three-magnon bound states turn out to exist only in the far corner of

the Brillouin zone. Since in the well-known one-dimensional cases the presence of longitudinal anisotropy favours the existence of bound states with lower total momentum, such anisotropy is included in our investigations. We find that if the anisotropy is greater than some critical value, three-magnon bound states of total momentum zero exist in the Heisenberg ferromagnet, and should therefore be observable in principle. Because the interaction that is responsible for the formation of bound states, becomes weaker if the magnetic moment of all ions is increased, we have only studied the case of spin one half, since the binding energies of bound states will be most pronounced in this case.

The organization of this paper is as follows. In the next section the integral equations, resulting from the application of Faddeev's formalism for the Dyson hamiltonian H_D are formulated and important symmetry properties will be discussed. The relatively simpler appearance of these equations, compared to those obtained from the Heisenberg spin hamiltonian H_S, has to be paid for by the presence of spurious dynamical features caused by the non-hermiticity and boson character of H_D. Analytic solution of the complete spectrum of H_D in one dimension[12]) learned that even spurious bound states can exist in the bound state regime of physical states. Fortunately the spurious part of the spectrum of H_D may be determined directly from the Schrödinger equation also in two dimensions. This will be the subject of section 3.

Then we are in a position to calculate all bound state energies from the Faddeev equations and decide whether they belong to physical or unphysical states. In section 4 the isotropic case will be treated, and the mere existence of bound complexes of three spin deviations will be established. In section 5 we shall investigate the behaviour of the bound states as a function of longitudinal anisotropy.

The discussions in section 4 and 5 are confined to the situation where the total momentum $\boldsymbol{P}$ is in the (1, 1) direction. In section 6 the results are extended to the case where $\boldsymbol{P}$ in general is not in the (1, 1) direction. Finally in the last section the possibility of experimentally observing these bound complexes is discussed.

2. The Faddeev equations

For definiteness, let us consider a two-dimensional simple cubic lattice of a large number N of spins $\frac{1}{2}$ with distance $\Delta = 1$ between neighbouring spins. The spins interact through nearest neighbour ferromagnetic exchange and longitudinal anisotropy is taken into account:

$$J_z \equiv J > 0, \qquad J_x = J_y = \sigma J \qquad (0 \leqslant \sigma \leqslant 1).$$

The hamiltonian is therefore:

$$H_S = -\tfrac{1}{2}J \sum_i \sum_\Delta [s_i^z s_{i+\Delta}^z + \sigma (s_i^x s_{i+\Delta}^x + s_i^y s_{i+\Delta}^y)]. \tag{2.1}$$

The operator $\bar{n} = \frac{1}{2}N + \Sigma_i s_i^z$ which gives the number of spin deviations from the totally aligned ground state $|0\rangle$ ($\bar{n} = 0$) commutes with H_S. One may therefore search for all energy eigenvalues within subspaces of states with definite $\bar{n}$. The problem of finding all bound state energies for $\bar{n} = 2$ has been solved extensively[4,5,13]). We shall here be concerned with the determination of all bound states for $\bar{n} = 3$ from the properties of the T-matrix.

In the case of $\bar{n} = 3$, integral equations for the T-matrix elements may be formulated within the framework of the Faddeev formalism[14]). However, taking H_S as a starting point for the derivation, one finds rather cumbersome equations owing to the restriction that only one spin deviation can occur at each lattice site. Therefore, in spite of the fact that the spin operators do not satisfy a definite boson or fermion statistics, H_S is replaced by the well-known Dyson hamiltonian[3])

$$H_D = \tfrac{1}{2}J \sum_i \sum_\Delta [a_i^+ a_i - a_i^+ a_i a_{i+\Delta}^+ a_{i+\Delta} - \sigma a_i^+ a_{i+\Delta} + \sigma a_i^+ a_{i+\Delta}^+ a_i^2], \tag{2.2}$$

where a_i^+ and a_i are creation and annihilation operators of bosons at site i.

Formally H_D can be obtained from eq. (2.1) by performing the Dyson–Maleev transformation[15]) to the spin operators $\vec{s}_i$:

$$s_i^+ = a_i^+, \qquad s_i^- = a_i - a_i^+ a_i a_i, \qquad s_i^z = -\tfrac{1}{2} + a_i^+ a_i .$$

As is well-known, this substitution rule is in accordance with the commutation rules for the spin operators, but violates the hermitean character of H_S. In the boson space the presence of one boson at site i is the analogue of one spin deviation at site i in real space. In the following the bosons will often loosely be called spin deviations. The number operator $n = \Sigma_i a_i^+ a_i$, the analogue of $\bar{n}$, commutes with H_D, so one may search for all eigenvalues of H_D within subspaces of definite n. As shown by Dyson, the complete spectrum of H_S is a subset of the spectrum of H_D, so that in principle we may use H_D as starting hamiltonian.

Let us now consider the equations for the T-matrix elements between states with three spin deviations. In the site representation the totally symmetric states are given by

$$|\boldsymbol{n}_1 \boldsymbol{n}_2 \boldsymbol{n}_3\rangle = a_{n_1}^+ a_{n_2}^+ a_{n_3}^+ |0\rangle \tag{2.3a}$$

with normalization

$$\langle \boldsymbol{n}_1' \boldsymbol{n}_2' \boldsymbol{n}_3' \mid \boldsymbol{n}_1 \boldsymbol{n}_2 \boldsymbol{n}_3\rangle = \sum_{P\binom{i_1 i_2 i_3}{1\,2\,3}} \delta_{n_{i_1}' n_1} \delta_{n_{i_2}' n_2} \delta_{n_{i_3}' n_3} \tag{2.3b}$$

and completeness relation

$$\tfrac{1}{6} \sum_{\substack{n_1 n_2 n_3 \\ \text{all}}} |\boldsymbol{n}_1 \boldsymbol{n}_2 \boldsymbol{n}_3\rangle \langle \boldsymbol{n}_1 \boldsymbol{n}_2 \boldsymbol{n}_3| = 1 . \tag{2.3c}$$

In momentum space totally symmetric three-magnon states are defined by

$$|\boldsymbol{k}_1\boldsymbol{k}_2\boldsymbol{k}_3\rangle = \frac{1}{N^{3/2}} \sum_{\substack{n_1 n_2 n_3 \\ \text{all}}} \exp(\mathrm{i}\boldsymbol{k}_1\boldsymbol{n}_1 + \mathrm{i}\boldsymbol{k}_2\boldsymbol{n}_2 + \mathrm{i}\boldsymbol{k}_3\boldsymbol{n}_3)\, a^+_{n_1} a^+_{n_2} a^+_{n_3} |0\rangle, \tag{2.4}$$

where $\boldsymbol{k}_1, \boldsymbol{k}_2, \boldsymbol{k}_3$ are the momenta of individual magnons, each of which is confined to the first Brillouin zone. These states obey normalization and completeness relations similar to (2.3b) and (2.3c).

The matrix elements of H_D between three-magnon states may be obtained from (2.2) by straightforward calculation, using (2.4) and the commutation rules for the creation and annihilation operators. There is a diagonal part

$$\langle \boldsymbol{k}_1\boldsymbol{k}_2\boldsymbol{k}_3| H_D^{(0)} |\boldsymbol{k}'_1\boldsymbol{k}'_2\boldsymbol{k}'_3\rangle = J \sum_{i=1}^{3} \sum_{d=x,y} (1 - \sigma \cos k_{id}) \langle \boldsymbol{k}_1\boldsymbol{k}_2\boldsymbol{k}_3 \mid \boldsymbol{k}'_1\boldsymbol{k}'_2\boldsymbol{k}'_3\rangle \tag{2.5}$$

and a non-diagonal part

$$\langle \boldsymbol{k}_1\boldsymbol{k}_2\boldsymbol{k}_3| V |\boldsymbol{k}'_1\boldsymbol{k}'_2\boldsymbol{k}'_3\rangle$$
$$= -(2J/N)\, \delta_{P,P'} \sum_{\Delta} \sum_{i,j=1}^{3} \cos \boldsymbol{p}_j \cdot \Delta\, (\cos \boldsymbol{p}'_i \cdot \Delta - \sigma \cos(\boldsymbol{K}'_i \cdot \Delta/2))\, \delta_{K_i', K_j}, \tag{2.6}$$

$$\boldsymbol{P} \equiv \boldsymbol{k}_1 + \boldsymbol{k}_2 + \boldsymbol{k}_3; \qquad \boldsymbol{K}_1 = \boldsymbol{k}_2 + \boldsymbol{k}_3, \qquad \boldsymbol{p}_1 = \tfrac{1}{2}(\boldsymbol{k}_2 - \boldsymbol{k}_3);$$

$$\boldsymbol{K}_2 = (\boldsymbol{k}_1 + \boldsymbol{k}_3), \qquad \boldsymbol{p}_2 = \tfrac{1}{2}(\boldsymbol{k}_3 - \boldsymbol{k}_1);$$

$$\boldsymbol{K}_3 = \boldsymbol{k}_1 + \boldsymbol{k}_2, \qquad \boldsymbol{p}_3 = \tfrac{1}{2}(\boldsymbol{k}_1 - \boldsymbol{k}_2),$$

$d = x, y$ are the two directions along the lattice sites. The non-diagonal part represents a two-body attractive interaction between magnons of momentum $\boldsymbol{k}_i$ and energy $J \Sigma_{d=x,y}(1 - \sigma \cos k_{id})$. Because of the separability of this interaction with respect to incoming and outgoing momenta, one can easily show that the three-magnon T-matrix elements have the following structure

$$\langle \boldsymbol{k}_1\boldsymbol{k}_2\boldsymbol{k}_3| T(E) |\alpha\rangle = \sum_{i=1}^{3} \sum_{d=x,y} \cos p_{id} \varphi_d^{(i)}(\boldsymbol{K}_i, E; \alpha), \tag{2.7}$$

where E represents the energy, α all parameters characterizing the incoming state. Application of the Faddeev formalism to the three-magnon bound state problem leads to a set of coupled integral equations in two continuous variables for the functions $\varphi_x^{(i)}$ and $\varphi_y^{(i)}$[8]. For completeness, a derivation of these equations is given in appendix I. In view of the total symmetry of the T-matrix (2.7) one readily can convince oneself that the functions $\varphi_x^{(i)}$ are identically the same. Similarly we only have one function $\varphi_y^{(i)}$. Hence the three-body equations simplify to a coupled set of integral equations for two functions φ_x and φ_y. In the following we shall

explicitly indicate the dependence on all variables and parameters relevant to the present discussion and omit all others for convenience. In order to write the equations in a clear manner, we introduce the following expressions (see appendix I)

$$N(K_x, K_y, K_x', K_y'; P_x, P_y)$$
$$= [3 - \tfrac{1}{2}E - \tfrac{1}{2}\sigma(\cos(P_x - K_x) + \cos(P_y - K_y))$$
$$- \sigma \cos \tfrac{1}{2}K_x \cos(P_x - K_x' - \tfrac{1}{2}K_x) - \sigma \cos \tfrac{1}{2}K_y \cos(P_y - K_y' - \tfrac{1}{2}K_y)]^{-1},$$

$$F_i(K_x, K_y, K_x', K_y'; P_x, P_y)$$
$$= \sum_{j=x,y} c_{ij}(K_x, K_y)(\cos(P_j - K_j' - \tfrac{1}{2}K_j) - \sigma \cos \tfrac{1}{2}K_j)$$
$$\times N(K_x, K_y, K_x', K_y'; P_xP_y) \qquad (i = x, y).$$

The functions c_{ij} containing the information of the two-magnon T-matrix, are discussed in appendix I. They obey the important symmetry property

$$c_{ij}(K_x, K_y) = c_{\bar{i}\bar{j}}(K_y, K_x) \tag{2.8}$$

in which $\bar{i}(\bar{j}) = y$ if $i(j) = x$; $\bar{i}(\bar{j}) = x$ if $i(j) = y$. Furthermore if we define

$$\mathscr{K}_{ij}(K_x, K_y, K_x', K_y'; P_x, P_y)$$
$$= \frac{1}{2\pi^2} F_i(K_x, K_y, K_x', K_y'; P_xP_y) \cos(K_j - P_j + \tfrac{1}{2}K_j') \quad (i = x, y; j = x, y), \tag{2.9}$$

then the Faddeev equations read

$$\varphi_x(K_x, K_y; P_x, P_y)$$
$$= \int_{-\pi}^{+\pi}\int \mathrm{d}K_x' \,\mathrm{d}K_y' [\mathscr{K}_{xx}(K_x, K_y, K_x', K_y'; P_x, P_y)\varphi_x(K_x', K_y'; P_x, P_y)$$
$$+ \mathscr{K}_{xy}(K_x, K_y, K_x', K_y'; P_x, P_y)\varphi_y(K_x', K_y'; P_y, P_y)], \tag{2.10a}$$

$$\varphi_y(K_x, K_y; P_x, P_y)$$
$$= \int_{-\pi}^{+\pi}\int \mathrm{d}K_x' \,\mathrm{d}K_y' [\mathscr{K}_{yx}(K_x, K_y, K_x', K_y'; P_x, P_y)\varphi_x(K_x', K_y'; P_x, P_y)$$
$$+ \mathscr{K}_{yy}(K_x, K_y, K_x', K_y'; P_x, P_y)\varphi_y(K_x', K_y'; P_x, P_y)]. \tag{2.10b}$$

From (2.8) and (2.9) the following symmetry properties are evident:

$$\mathscr{K}_{ij}(K_x, K_y, K_x', K_y'; P_x, P_y) = \mathscr{K}_{\bar{i}\bar{j}}(K_y, K_x, K_y', K_x'; P_y, P_x), \tag{2.11}$$

where the indices $\bar{i}, j$ have the meaning explained below (2.8). Introducing these properties of $\mathscr{K}_{ij}$ into (2.10) one observes that the solutions φ_x and φ_y fall into two symmetry classes S_0 and A_0 respectively defined by

$$S_0\colon\ \varphi_x(K_x, K_y; P_x, P_y) = \varphi_y(K_y, K_x; P_y, P_x), \tag{2.12a}$$

$$A_0\colon\ \varphi_x(K_x, K_y; P_x, P_y) = -\varphi_y(K_y, K_x; P_y, P_x). \tag{2.12b}$$

The existence of such symmetries represents a special feature of the cubic structure of the reciprocal lattice. In one special situation eqs. (2.10) can be simplified further. Namely, in the (1, 1) direction, *i.e.* $P_x = P_y = P$, eqs. (2.12) relate φ_x and φ_y at the same value of total momentum $\boldsymbol{P}$; in this case the integral equations are decoupled into equations for φ_x and φ_y alone

$$\varphi_x(K_x, K_y; P, E) = \int_{-\pi}^{+\pi}\int \mathrm{d}K_x'\,\mathrm{d}K_y' \,[\mathscr{K}_{xx}(K_x, K_y, K_x', K_y'; P, E) \pm \mathscr{K}_{xy}(K_x, K_y, K_y', K_x'; P, E)]\,\varphi_x(K_x', K_y'; P, E), \tag{2.13}$$

where the positive sign in the kernel corresponds to S_0-solutions, and the negative sign to A_0-solutions. Similar equations hold for φ_y.

3. Unphysical states

In general no analytic solutions for the bound state energies can be found for equations (2.13). However, various successful numerical methods may be employed to determine the location of three-magnon bound states. These methods will be described in detail in the next section, where the first numerical results are given.

The Faddeev equations may be examined analytically somewhat further, particularly with respect to the Ising limit. Since this mainly serves as check on the numerical results, it will be presented together with the calculations. We first turn to the evaluation of the unphysical states.

Since the equations of the previous section have been formulated on the basis of the Dyson hamiltonian, they have also solutions corresponding to unphysical states. The energy spectrum of these states can be determined directly from the Schrödinger equation. These results allow us to discriminate between the physical and unphysical states which are found from the Faddeev equations. Let a

general state with three spin deviations be given as

$$|\psi\rangle = \sum_{\substack{n_1 n_2 n_3 \\ \text{all}}} a_{n_1 n_2 n_3} |\boldsymbol{n}_1 \boldsymbol{n}_2 \boldsymbol{n}_3\rangle. \tag{3.1}$$

The Schrödinger equations for the amplitudes $a_{n_1 n_2 n_3}$ in a two-dimensional square lattice are given by

$$\begin{aligned}(E - 6)\, a_{n_1 n_2 n_3} = & -\tfrac{1}{2}\sigma \sum_{\Delta} (a_{n_1 - \Delta n_2 n_3} + a_{n_1 n_2 - \Delta n_3} + a_{n_1 n_2 n_3 - \Delta}) \\ & + \tfrac{1}{2} \sum_{\Delta} \delta_{n_1 n_2 + \Delta} (\sigma a_{n_3 n_1 n_1} + \sigma a_{n_3 n_2 n_2} - 2a_{n_1 n_2 n_3}) \\ & + \tfrac{1}{2} \sum_{\Delta} \delta_{n_1, n_3 + \Delta} (\sigma a_{n_2 n_1 n_1} + \sigma a_{n_2 n_3 n_3} - 2a_{n_1 n_2 n_3}) \\ & + \tfrac{1}{2} \sum_{\Delta} \delta_{n_2, n_3 + \Delta} (\sigma a_{n_1 n_2 n_2} + \sigma a_{n_1 n_3 n_3} - 2a_{n_1 n_2 n_3}).\end{aligned} \tag{3.2}$$

Here we have put $J = 1$, as will be done from now on. These are easily obtained by straightforward calculation of

$$\langle \boldsymbol{n}_1 \boldsymbol{n}_2 \boldsymbol{n}_3 |\, H_{\mathrm{D}}\, |\psi\rangle = E \langle \boldsymbol{n}_1 \boldsymbol{n}_2 \boldsymbol{n}_3 \mid \psi\rangle.$$

For physical states it is not convenient to treat eqs. (3.2) any further. However, for unphysical states a tremendous simplification occurs since all physical amplitudes $a_{n_1 n_2 n_3}$ ($\boldsymbol{n}_1 \neq \boldsymbol{n}_2 \neq \boldsymbol{n}_3 \neq \boldsymbol{n}_1$) are zero by definition. The general equation for all $a_{n_1 n_1 n_3}$ of unphysical states is therefore

$$\begin{aligned}(E - 6)\, a_{n_1 n_1 n_3} = & -\tfrac{1}{2}\sigma \sum_{\Delta} (2a_{n_1 - \Delta n_1 n_3} + a_{n_1 n_1 n_3 - \Delta}) \\ & + \sum_{\Delta} \delta_{n_1, n_3 + \Delta} (\sigma a_{n_1 n_1 n_1} + \sigma a_{n_1 n_3 n_3} - 2a_{n_1 n_1 n_3})\end{aligned} \tag{3.3}$$

or considering the different cases, putting all physical amplitudes that may occur equal to zero, and denoting

$a_{n_1 n_1 n_3}$ as $c_{n_1}(\boldsymbol{n}_3)$, we find

$$(E - 6)\, c_{n_1}(\boldsymbol{n}_3) + \tfrac{1}{2}\sigma \sum_{\Delta} c_{n_1}(\boldsymbol{n}_3 + \Delta) = 0 \tag{3.4a}$$

if $\boldsymbol{n}_3$ is no neighbour of $\boldsymbol{n}_1$.

$$(E - 4)\, c_{n_1}(\boldsymbol{n}_3) = \sigma c_{n_1}(\boldsymbol{n}_1) - \tfrac{1}{2}\sigma \sum_{\Delta} c_{n_1}(\boldsymbol{n}_3 + \Delta) \tag{3.4b}$$

if $\boldsymbol{n}_3 = \boldsymbol{n}_1 + \boldsymbol{\Delta}'$, $\boldsymbol{\Delta}'$ being a nearest neighbour vector of $\boldsymbol{n}_1$.

$$(E - 6)\, c_{n_1}(\boldsymbol{n}_1) + \tfrac{3}{2}\sigma \sum_{\boldsymbol{\Delta}} c_{n_1}(\boldsymbol{n}_1 + \boldsymbol{\Delta}) = 0 \tag{3.4c}$$

if $n_3 = n_1$.

In view of translational symmetry the general form of the solution to eqs. (3.4) is given by

$$c_{n_1}(\boldsymbol{n}_3) = \mathrm{e}^{\mathrm{i}\boldsymbol{P}\cdot\boldsymbol{n}_1}\, \gamma\,(|\boldsymbol{n}_3 - \boldsymbol{n}_1|),$$

where $\boldsymbol{P}$ is the total momentum of the complex, the possible values of which are determined by periodic boundary conditions. Putting $a \equiv E - 6$ and $b \equiv E - 4$ we obtain from eqs. (3.4)

$$a\gamma\,(|\boldsymbol{n}_3 - \boldsymbol{n}_1|) + \tfrac{1}{2}\sigma \sum_{\boldsymbol{\Delta}} \gamma\,(|\boldsymbol{n}_3 - \boldsymbol{n}_1 + \boldsymbol{\Delta}|) = 0, \tag{3.5a}$$

$$b\gamma\,(|\boldsymbol{\Delta}'|) - \sigma\gamma\,(0) + \tfrac{1}{2}\sigma \sum_{\boldsymbol{\Delta}} \gamma\,(|\boldsymbol{\Delta}' + \boldsymbol{\Delta}|) = 0, \tag{3.5b}$$

$$a\gamma\,(0) + \tfrac{3}{2}\sigma \sum_{\boldsymbol{\Delta}} \gamma(|\boldsymbol{\Delta}|) = 0. \tag{3.5c}$$

From these equations the energy eigenvalues of all unphysical states follow, and since the total momentum $\boldsymbol{P}$ does not occur in the equations, all these energies are independent of $\boldsymbol{P}$. This important property was also found to be valid in one dimension[12]).

TABLE I

The energies E_{B1}, E_{B2}, E_{B3} of the unphysical bound states at $\sigma = 1$ in a finite square lattice of N^2 spins with periodic boundary conditions. (See also ref. 26.)

$[N \times N]$	E_{B1}, E_{B2}	E_{B3}
5×5	3.6501	3.8193
6×6	3.6214	3.8399
7×7	3.6121	3.8473
8×8	3.6088	3.8502
9×9	3.6076	3.8515
10×10	3.6071	3.8521

The position of the energy levels may be obtained numerically by considering a finite lattice with periodic boundary conditions. One calculates the eigenvalues λ_i of the homogeneous system of equations (3.5) as a function of energy. Each $E_i^{(0)}$ with $\lambda_i(E_i^{(0)}) = 0$ corresponds to an energy level of the system. Two of the obtained eigenvalues are complex, which is caused by the non-hermiticity of H_D,

most of the others give rise to the continuum of unphysical scattering states for $N \to \infty$, representing the scattering of one magnon of energy $\Sigma_{i=x,y}(1 - \sigma \cos k_i)$ from the unphysical two-magnon bound state at $E = 4$. As a result this continuum ranges from $6 - 2\sigma$ to $6 + 2\sigma$. The zeros of four of the eigenvalues are below the bottom of this continuum, thus being unphysical bound states of the system.

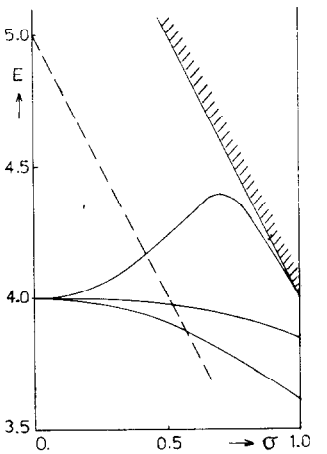

Fig. 1. Unphysical bound state curves as a function of anisotropy σ. The shaded line indicates the bottom of the unphysical continuum, the dashed line that of the physical continuum. The energy is given in units of J.

On increasing the number of spins in the lattice, there is rapid convergence in the position of these levels as shown in table I for the bound state energies at $\sigma = 1$. In fig. 1 the bound state energies are shown as a function of σ together with the bottom of the band of unphysical scattering states. The lowest level is doubly degenerate for all values of σ, which can be understood from symmetries to be discussed in section 5. The dashed curve indicates part of the bottom of the band of physical three-magnon states at $P_x = P_y = \pi$ (a special case that we shall study later). To the left of this curve the unphysical bound states enter the bound state regime of physical states at $P_x = P_y = \pi$. In the Ising limit, $\sigma \to 0$, there is a fourfold degenerate level at $E = 4$, corresponding to the four eigenstates $|\psi_\Delta\rangle = e^{iP\cdot n}|n, n, n + \Delta\rangle$ at $E = 4$ in that limit.

4. The isotropic case

In this section we consider the isotropic case, $\sigma = 1$, and confine our attention to states with total momentum in the (1, 1) direction. Some of the results of this section have already appeared in a letter[16]). In this case the existence of three-

magnon bound states may be investigated by determining numerically whether equations (2.13) allow for solutions at real values of the energy parameter E below the bottom of the band of three-magnon scattering states. The results are summarized in fig. 2. One sees that three-magnon bound states, represented by solid lines, indeed exist, if the total momentum variable $P = P_x = P_y$ is large enough.

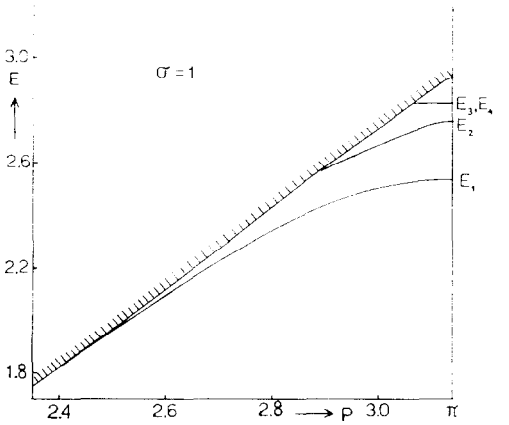

Fig. 2. The energy E of three-magnon bound states in the (1, 1) direction (solid lines) as a function of total momentum P at $\sigma = 1$. The bottom of the band is indicated by a shaded line.

The shaded line indicates the bottom of the band of states in which one free magnon is scattered by a two-magnon bound state (see appendix II). In table II the calculated energies and binding energies (within parentheses) at $P = \pi$ of all bound states are given, together with their symmetry as defined by eqs. (2.12).

TABLE II

The energy in units of J for the bound states at $\sigma = 1$ and $P_x = P_y = \pi$. The symmetry of the states is indicated according to the notation of eqs. (2.12). The errors in the numbers are estimated to be a few parts of a percent.

Level	Symmetry	Energy (binding energy)
E_1	S_0	2.53 (0.40)
E_2	S_0	2.76 (0.17)
E_3	A_0	2.83 (0.10)
E_4	S_0	2.83 (0.10)

E_3 and E_4 are exactly degenerate at $P = \pi$, a property that will be proved analytically for this level at all values of σ in the next section. For $P \lesssim \pi$ the degeneracy is lifted, but the actual splitting of the levels in their range of existence is too small to be drawn in the figure. According to table I all states are physical bound states. Notice that only a small part of the Brillouin zone has been shown in fig. 2, and that all bound states lie in the corner of the zone. As a consequence there is little hope to find the three-magnon bound states experimentally in an isotropic Heisenberg ferromagnet.

Let us now describe in some detail the numerical methods that lead to these results. In all the methods gaussian quadratures have been employed with up to 16 meshpoints in each variable. By varying the number of meshpoints the numerical error was estimated to be less than 0.5%.

The first method consists of determining the zeros of $\det(1 - K)$ where K is the kernel of the integral equation. In most calculations, however, a different method has been used, namely all eigenvalues and eigenvectors of K have been determined. The bound state energies are then simply found from the eigenvalues $\lambda(E) = 1$. This method has the advantage of allowing us for a classification of the bound state energies according to the symmetries of the corresponding eigenvectors. In the cases that both methods have been used agreement was found.

In practice the above methods can only be used if the matrices involved are of limited size. In particular, for the calculations with the total momentum not in the (1, 1) direction the matrices become too large to be dealt with by the above techniques. In this case the method was used of calculating the padé approximants to φ_x and φ_y. Adding the inhomogeneous term to eqs. (2.10) [see appendix I, eq. (I.11)], one formally obtains the following equations.

$$\varphi_x(\lambda, E) = \varphi_x^{(0)} + \lambda\{\mathscr{K}_{xx}(E)\,\varphi_x(\lambda, E) + \mathscr{K}_{xy}(E)\,\varphi_y(\lambda, E)\}, \tag{4.1}$$

$$\varphi_y(\lambda, E) = \varphi_y^{(0)} + \lambda\{\mathscr{K}_{yx}(E)\,\varphi_x(\lambda, E) + \mathscr{K}_{yy}(E)\,\varphi_y(\lambda, E)\}, \tag{4.2}$$

where we have introduced for convenience a complex parameter λ in front of the kernels of the integral equations. Of course $\lambda = 1$ in actual calculations. By iterating eqs. (4.1) and (4.2) one obtains perturbation expansions for φ_x and φ_y which are generally not converging

$$\varphi_x(\lambda, E) = \sum_n \lambda^n \varphi_x^{(n)}(E), \tag{4.3a}$$

$$\varphi_y(\lambda, E) = \sum_n \lambda^n \varphi_y^{(n)}(E). \tag{4.3b}$$

One can, however, calculate the diagonal $[N, N]$ Padé approximants in λ to φ_x and φ_y, given by

$$\varphi_i^{[N,N]}(\lambda, E) = P_i^{(N)}(\lambda, E)/Q_i^{(N)}(\lambda, E) \qquad (i = x, y),$$

where $P_i^{(N)}$ and $Q_i^{(N)}$ are Nth order polynomials in λ, the coefficients of which can be determined from $\varphi_x^{(n)}$ and $\varphi_y^{(n)}$. One knows[17]) that

$$\lim_{N\to\infty} \varphi_i^{[N,N]}(\lambda, E) = \varphi_i(\lambda, E) \qquad (i = x, y).$$

The coefficients $\varphi_x^{(n)}$ and $\varphi_y^{(n)}$ of eqs. (4.3) may readily be calculated by successive iteration of equation (2.10). The important question with respect to the applicability of the method is whether the Padé approximants converge fast enough to their values $\varphi_i^{[\infty,\infty]}$, otherwise too many iterations have to be performed. For our problem the rate of convergence is reasonable and generally a [9, 9] approximant is sufficient to obtain convergence. From the poles of the Padé approximants in the energy variable, the bound state energies follow again. In this way these energies were explicitly calculated in the (1, 1) direction, and the results of table II are reaffirmed, which demonstrates the applicability of the method. Finally we mention a property that may be very useful sometimes. The expansion coefficients of eqs. (4.3) obey the relation[18]).

$$\lim_{n\to\infty} \frac{\varphi_i^{(n+1)}(E)}{\varphi_i^{(n)}(E)} = \frac{1}{\lambda_0(E)}, \tag{4.4}$$

where $\lambda_0(E)$ is the pole of $\varphi_i(\lambda, E)$ closest to the origin of the λ-plane. By determining E_0 such that $\lambda_0(E_0) = 1$, the physical value of λ, one has obtained the state with lowest possible energy E_0, in this case the lowest lying three-magnon bound state. By applying (4.4) one may therefore rigorously confine the area where one has to search for bound states with one of the described methods.

5. The anisotropic case

Since experimental observation of three-magnon bound states seems hardly conceivable for the isotropic ferromagnet, we now consider the properties of bound states when longitudinal anisotropy, $0 \leqslant \sigma < 1$, is taken into account. Let us first discuss the Ising limit. One has for every value of the total momentum $\boldsymbol{P}$ one level of six states of type $e^{i\boldsymbol{P}\cdot\boldsymbol{n}}|\boldsymbol{n}, \boldsymbol{n} + \boldsymbol{\Delta}_0, \boldsymbol{n} + \boldsymbol{\Delta}_1\rangle$ at energy $E = 4$. Here $\boldsymbol{\Delta}_0$ and $\boldsymbol{\Delta}_1$ are different nearest neighbour vectors of site $\boldsymbol{n}$. It is to be expected that these states represent the three-magnon bound states in this limit. Furthermore we have a large number of states $e^{i\boldsymbol{P}\cdot\boldsymbol{n}}|\boldsymbol{nn} + \boldsymbol{\Delta m}\rangle$, where $\boldsymbol{m}$ is no neighbour of $\boldsymbol{n}$ or $\boldsymbol{n} + \boldsymbol{\Delta}$, which represent the band of states of two bound magnons and one free magnon collapsed into one highly degenerate level at $E = 5$. From these considerations and the results on the isotropic case one may beforehand guess what happens in the range $0 < \sigma < 1$. We expect the binding energy of bound states to increase as σ decreases. Furthermore it is expected that, when σ decreases,

gradually more bound states will exist down to $\boldsymbol{P} = 0$, since for $\sigma = 0$ six bound states exist at $\boldsymbol{P} = 0$. Finally one may conjecture that two bound states have to emerge from the continuum at some values of σ, because there is a sixfold degenerate level in the Ising limit and only four bound states in the isotropic case. After this qualitative discussion we now present our results on the (1, 1) direction. In obtaining the bulk of these results we used the second numerical method described in section 4. However, to feel sure of its applicability over the whole range

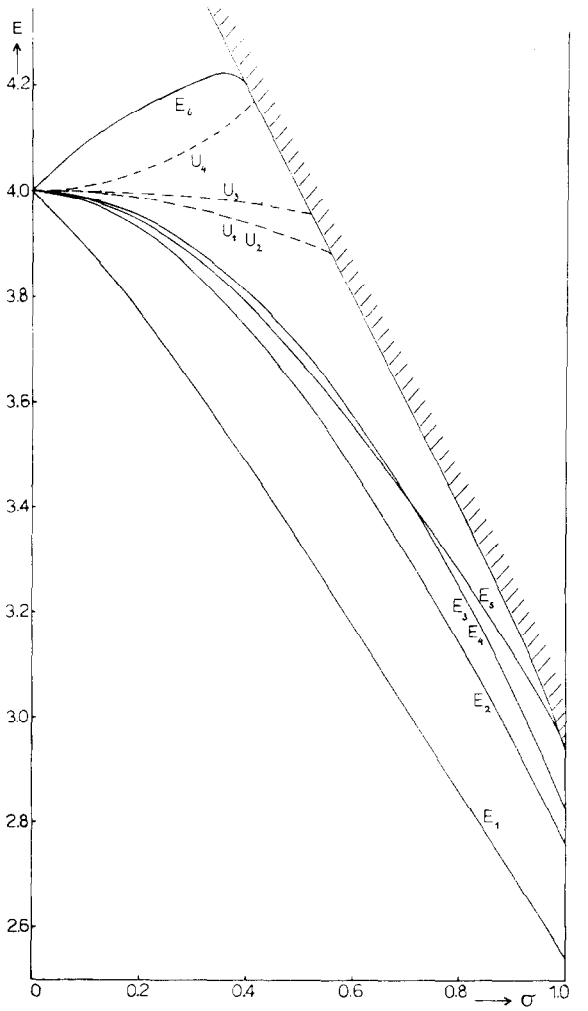

Fig. 3. All energies of three-magnon bound states (physical ones indicated by E_i, unphysical ones by U_i) in the (1, 1) direction at $P = \pi$ as a function of σ. The shaded line indicates the bottom of the band.

of values of σ, we compared the results at $\sigma = 0.10, 0.25$ and 0.50 with those obtained from Padé approximants, and found excellent agreement. In order not to digress from our main results, we shall give an account of calculations on the band structures appearing in the figures in appendix II.

5.1. *Results at* $P = \pi$

Let us first look at that point of the first Brillouin zone where the presence of bound states is expected to be most prominent, *i.e.*, $P = P_x = P_y = \pi$. In fig. 3 the bound state energies are shown as a function of σ. The shaded line corresponds to the bottom of the three-magnon band. At $\sigma = 1$ we have the bound state energies of table II. From our analysis of section 3 we know that the dashed bound state curves of fig. 3 correspond to unphysical bound states. The fact that there is complete agreement with the results of section 3 – also the degeneracy of U_1 and U_2 is found numerically – is an important check on the correctness of our calculations. It should be noted from fig. 3 that the bottom of the band is given by a straight line up to $\sigma = 0.8$ (see appendix II). As we already conjectured, the binding energy of all bound states increases as σ decreases, and the levels E_5 and E_6, which are not present at $\sigma = 1$, branch off from the continuum at $\sigma \approx 1$ and $\sigma \approx 0.4$, respectively. In the Ising limit the bound states form a tenfold degenerate level of six physical states, mentioned at the beginning of this section, and four unphysical states discussed at the end of section 3. Moreover, one may perform simple perturbation theory on $H_0 = -\frac{1}{2}\Sigma_i \Sigma_\Delta s_i^z s_{i+\Delta}^z$ with $V = -\frac{1}{2}\sigma \Sigma_i \Sigma_\Delta (s_i^x s_{i+\Delta}^x + s_i^y s_{i+\Delta}^y)$ as a perturbation, for the sixfold degenerate level of physical states. As a result one finds that two energies shift like $4 + \sigma$ and $4 - \sigma$ respectively, while the other four are not affected in lowest order. The calculated results are in agreement with this fact.

Let us now examine the integral equations closer, to see whether more symmetries are present at $P = \pi$ than those discussed in section 2. We write the equations for φ_x explicitly at $P = \pi$:

$$\varphi_x(x', y') = \frac{1}{2\pi^2} \int_{-\pi}^{+\pi}\int \mathrm{d}x\, \mathrm{d}y \{[c_{xx}(\cos(x + \tfrac{1}{2}x') + \beta_x) + c_{xy}(\cos(y + \tfrac{1}{2}y') + \beta_y)]$$

$$\times (t + \beta_x \cos(x + \tfrac{1}{2}x') + \beta_y \cos(y + \tfrac{1}{2}y'))^{-1}\}$$

$$\times \{\cos(x' + \tfrac{1}{2}x)\, \varphi_x(x, y) \pm \cos(y' + \tfrac{1}{2}y)\, \varphi_x(y, x)\}. \qquad (5.1)$$

We have put x, y instead of K_x, K_y *etc.*, $\beta_x \equiv \sigma \cos x'/2$, $\beta_y \equiv \sigma \cos y'/2$, $t = 3 - E/2 + \sigma/2(\cos x' + \cos y')$. The positive sign applies to S_0-symmetry: $\varphi_x(x, y) = \varphi_y(y, x)$, the negative sign to A_0-symmetry: $\varphi_x(x, y) = -\varphi_y(y, x)$. We note from the definition of β_x, β_y and (I.3–5) that $c_{ij}(x, y) = c_{ij}(-x, -y)$. It is then

easy to see from (5.1), by changing the integration variable x into $-x$ and y into $-y$, that both S_0- and A_0-solutions fall into two classes S_1 and A_1:

$$S_1: \quad \varphi_x(x, y) = \varphi_x(-x, -y), \tag{5.2a}$$

$$A_1: \quad \varphi_x(x, y) = -\varphi_x(-x, -y). \tag{5.2b}$$

Furthermore eqs. (5.1) allow solutions of S_0, S_1 and A_0, S_1 type to have the following symmetry in each of the variables

$$S_2: \quad \varphi_x(x, y) = \varphi_x(-x, y) = \varphi_x(x, -y), \tag{5.3a}$$

$$A_2: \quad -\varphi_x(x, y) = \varphi_x(-x, y) = \varphi_x(x, -y). \tag{5.3b}$$

Solutions of S_0, A_1 and A_0, A_1 type do not have such symmetries. However, if there exists a solution of S_0, A_1 type, then one may readily convince oneself from (5.1) by changing the integration variables appropriately that at the same energy we also have a solution of A_0, A_1 symmetry given by

$$\varphi_x^{(A_0, A_1)}(x, y) = \varphi_x^{(S_0, A_1)}(-x, y). \tag{5.4}$$

From fig. 3 one sees that indeed two such twofold degenerate levels exist. In each level equality in eight decimals was obtained for the energies of both states, which is convincing enough to establish exact degeneracy. Since also the eigenvectors have been calculated, we may classify all bound state energies according to the symmetries (2.12) and (5.2)–(5.3) of the corresponding eigenfunctions (see table III).

TABLE III

The symmetries as defined by eqs. (2.12), (5.2) and (5.3) of all states corresponding to the energies of fig. 3. The solutions φ_x and φ_y to the Faddeev equation at $\sigma = 0$, which can be obtained analytically, are also given.

Level	Symmetry	φ_x	φ_y
E_1	$S_0\ S_1\ A_2$	$\sin(\frac{1}{2}x)\sin(y)$	$\sin(\frac{1}{2}y)\sin(x)$
E_2	$S_0\ S_1\ S_2$	$\cos(3x/2)$	$\cos(3y/2)$
E_3	$A_0\ A_1$	$-\sin(\frac{1}{2}x + y)$	$\sin(\frac{1}{2}y + x)$
E_4	$S_0\ A_1$	$\sin(\frac{1}{2}x - y)$	$\sin(\frac{1}{2}y - x)$
E_5	$A_0\ S_1\ S_2$	$\cos(3x/2)$	$-\cos(3y/2)$
U_1	$A_0\ A_1$	$-\sin(\frac{1}{2}x)$	$\sin(\frac{1}{2}y)$
U_2	$S_0\ A_1$	$\sin(\frac{1}{2}x)$	$\sin(\frac{1}{2}y)$
U_3	$A_0\ S_1\ S_2$	$\cos(\frac{1}{2}x)$	$-\cos(\frac{1}{2}y)$
U_4	$S_0\ S_1\ S_2$	$\cos(\frac{1}{2}x)$	$\cos(\frac{1}{2}y)$
E_6	$S_0\ S_1\ S_2$	$\cos(\frac{1}{2}x)\cos(y)$	$\cos(\frac{1}{2}y)\cos(x)$

This classification constitutes another important check on the reliability of our numerical results. It holds for all σ. For $P < \pi$, however, the properties (5.2)–(5.4) break down, in particular E_3 and E_4 are not degenerate anymore as can be seen from figs. 4 and 5.

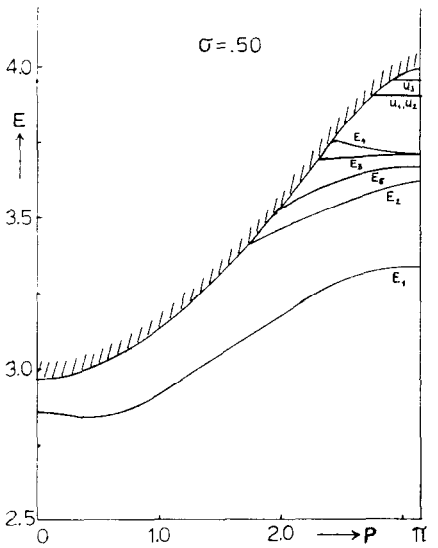

Fig. 4

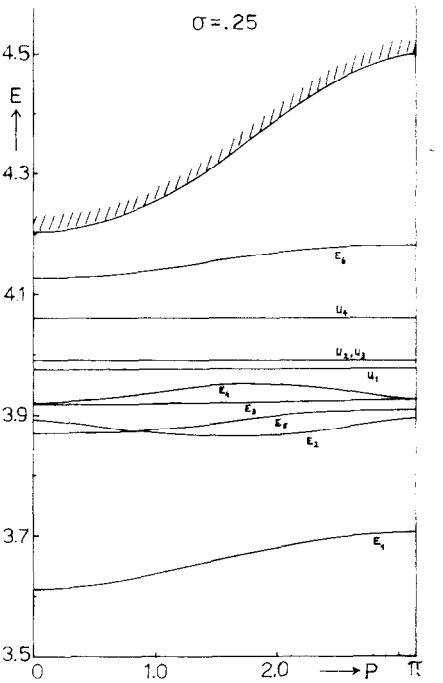

Fig. 5

Fig. 4. All three-magnon bound state energy curves in the (1, 1) direction as a function of P at $\sigma = 0.50$. The shaded line represents the bottom of the band.
Fig. 5. The same as fig. 4, except that $\sigma = 0.25$.

5.2. *Results for* $P < \pi$

In order to discuss the behaviour of three-magnon bound state energies as a function of total momentum at various values of σ, we have calculated all bound state energies in the range $0 \leqslant P \leqslant \pi$ for two typical values of σ, namely $\sigma = 0.25$ and $\sigma = 0.50$. The results are shown in figs. 4 and 5. The shaded lines indicate the position of the bottom of the three-magnon band (see appendix II). The figures show that the binding energy of each bound state increases, at any value of P where it exists, as σ decreases. Quite on line with this effect, bound states exist at lower values of P if σ becomes smaller, and thus gradually more bound states exist down to $P = 0$.

At $\sigma = 0.50$ this is the case for the lowest lying state, at $\sigma = 0.25$ already all bound states exist at $P = 0$. From an experimental point of view this means that in these cases bound states become measurable in principle, since all conceivable experimental techniques probe the region $P \approx 0$. Therefore in fig. 6 the binding energy at $P = 0$ as a function of σ has been drawn. We see that only in materials where σ is well below 0.55 there is any hope of measuring three-magnon bound states. The behaviour of bound states in other directions than the (1, 1) direction does not affect this conclusion, as we shall see in the next section. The shaded area in fig. 6 indicates the region in which all other binding energies occur, they have

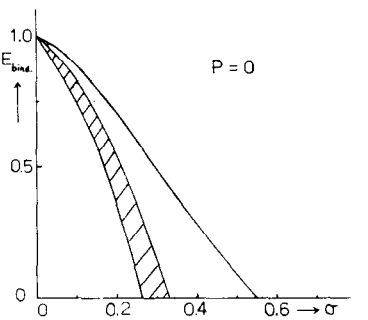

Fig. 6. Binding energy at $P = 0$ as a function of σ of the lowest lying bound state (curve) and of all other bound states (shaded area).

not been calculated precisely for every individual bound state. From figs. 4 and 5 we see further that all physical bound states show dispersion, and that the degree of dispersion decreases with σ such that in the Ising limit no dispersion is left and $E = 4$ at all values of P. The unphysical states, however, are found to be dispersionless, as they should be according to our results of section 3, and U_1 and U_2 are exactly degenerate at all values of P.

6. Bound states in different directions

Let us now investigate the existence of bound states that do not have their total momentum in the (1, 1) direction, $P_x \neq P_y$. In this case the bound state energies have to be determined from Padé approximants, as described in section 4, since the previously applied method cannot be used because of the size of the resulting matrices. In as far as we are interested only in the rather qualitative aspects of the behaviour of bound states in different directions, we shall only consider the lowest lying bound state energy for which results may be obtained very economically by means of (4.4).

1) In fig. 7 we have drawn the resulting bound state spectrum for $\sigma = 1$ at $P_y = \alpha P_x = \alpha P$ as a function of P for $\alpha = 0.90$. To clarify what happens the bottom of the band together with the lowest bound state energy curve has been drawn for $\alpha = 1$ (dashed lines). As one sees, in taking the direction $\alpha = 0.90$ the bottom of the bands drops considerably while the change in the bound state energies in the neighbourhood of $P = \pi$ is relatively small. Consequently the binding energy at each value of P is smaller for $\alpha = 0.90$ than for $\alpha = 1$. E_3 and E_4 have already disappeared. We might conjecture that further away from the (1, 1) direction bound states do not even exist. This is indeed the case as may be

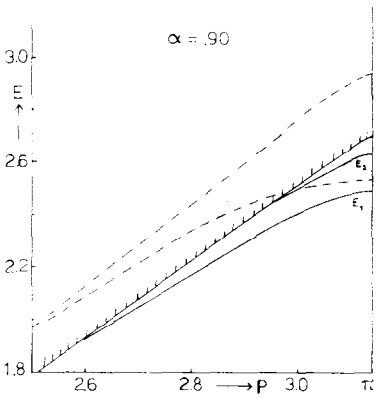

Fig. 7. Bound state energy curves at $\sigma = 1$ in the direction $P_y/P_x = 0.90$ as a function of $P_x = P$. For comparison the bottom of the band and the lowest lying bound state at $P_y/P_x = 1$ are also shown (dashed lines).

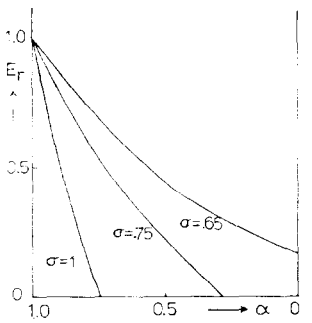

Fig. 8

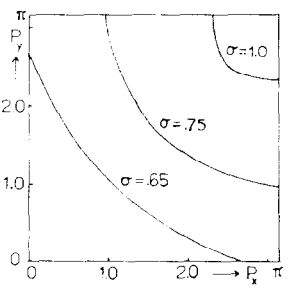

Fig. 9

Fig. 8. Binding energy at $P_y = \alpha\pi$, $P_x = \pi$ as a function of α for various values of σ. The ratio of the binding energy at α and at $\alpha = 1$ has been plotted (E_r).

Fig. 9. Region of the brillouin zone in which at least one and no bound state exists respectively, at various values of σ. No bound states exist in the region bounded by the curve corresponding to a particular σ and including the point $P = 0$.

seen from figs. 8 and 9. Both figures relate to the lowest bound state energy curve only, since we are more interested in qualitative features, than in the detailed behaviour of all bound state energies. In fig. 8 we have plotted, at various values of σ, the binding energy at the point where it has its greatest value, $P_x = \pi$, $P_y = \alpha\pi$, relative to the binding energy at $P_x = P_y = \pi$. In fig. 9 the regions of the Brillouin zone are indicated, where at least one bound state and no bound states exist respectively, for some values of σ. In the isotropic case for $\alpha \lesssim 0.74$ no bound states exist anymore (figs. 8, 9). Moreover we see from fig. 9 that for $\alpha < 1$ the neighbourhood of $P = \pi$ in which bound states occur decreases with α.

2) Taking longitudinal anisotropy into account, we have for fairly small anisotropy ($\sigma = 0.75$ in figs. 8 and 9) similar behaviour as in the isotropic case. But the region where at least one bound state exists is growing rapidly as the anisotropy increases, until finally one or more bound states exist in all directions. At the same time the rate of decrease of the binding energy as α goes from one to zero becomes smaller with σ, but at all values of σ the binding energy remains at its maximum for $\alpha = 1$. Finally, as soon as a bound state exists at $P = 0$ for $\alpha = 1$, it exists in every direction, however, with a smaller binding energy. From an experimental point of view we may now complete our discussion of the previous section by stating that the most favourable conditions to try and observe three-magnon bound states are found in anisotropic materials with σ well below 0.55 by searching in the (1, 1) direction.

7. Concluding remarks

We have calculated all bound state energy curves of three magnons for the isotropic and longitudinally anisotropic Heisenberg ferromagnet. The kinematical restriction that only one spin deviation ($s = \frac{1}{2}$) can occur at each lattice site has been circumvented by using Dyson's hamiltonian. We have demonstrated that the spurious features of the spectrum of this hamiltonian can be dealt with explicitly in the three-magnon subspace. Therefore the physical part of the spectrum can be isolated from the unphysical part, which makes Dyson's hamiltonian useful in determining the bound state spectrum of the Heisenberg spin system. However, apart from the spectrum not much correct information on dynamical features can be obtained from Dyson's hamiltonian. Already the three-magnon bound state wave functions are incorrect[12]), which was pointed out for two-magnon bound states earlier[19]). Also with respect to scattering cross sections of three-magnon states, generally the Dyson hamiltonian will give wrong results, except may be in the limit of all magnons involved having very long wavelengths, as may be inferred from results on two-magnon states[3,20]).

In order to obtain our results we have applied Faddeev's formalism to three interacting magnons. In one dimension this was first done by Majumdar[8]) who

regained numerically Bethe's result for the three-magnon bound state energy. Later we showed[12]) that in the one dimensional case a complete analytic solution can be given, which shows great similarity with analytic solutions obtained for three particles interacting pairwise through delta function potentials[21,22]), this in spite of the fact that the dispersion relations, p^2 *versus* $1 - \cos k$, and the potentials are very different in both cases. Unfortunately in two dimensions analytic solutions of the kind seem hard to obtain. However, it has been demonstrated in this paper that substantial information on three-magnon states can be obtained numerically. Finally, some attention has to be paid to the experimental possibilities of measuring three-magnon bound states. In discussing experiment so far, we were referring to infrared absorption measurements, that were so successful in detecting multiple magnon bound states in the one-dimensional salt $CoCl_2 \cdot 2H_2O$[2]). For such experiments, however, the presence of transverse anisotropy is crucial[1,2]). If such anisotropy is included the number of spin deviations is not a conserved quantity, to the effect that three-magnon states are mixed into the one-magnon states and thereby become optically observable. The treatment of this paper relies heavily upon the fact that the total number of spin deviations is a conserved quantity, and therefore transverse anisotropy has not been included. In order to confirm our results experimentally, one should therefore find a two-dimensional sample in which enough transverse anisotropy is present, to make experiments possible, but at the same time so little that it can be treated perturbatively like in $CoCl_2 \cdot 2H_2O$[1,2,10]), and that the results of this paper are true in lowest order. Apart from this optical experiment, two other candidates for measuring three-magnon bound states should be mentioned. The dispersion curves of magnons or phonons might intersect the dispersion curves of three-magnon bound states (or their continuation as resonances). In that case the magnon–magnon and magnon–phonon interaction respectively may have an anomalous effect on the energies and lifetimes of respectively magnons and phonons. A theoretical treatment like in the case of two-magnon bound states[23,24]) seems quite conceivable. However, to our knowledge such anomalies have not yet been observed. Thinking, however, of recent developments[25]) in the preparation of monochromatic phonons of given momentum and polarization, we feel that it might be promising to search for bound states experimentally along these lines.

Appendix I

In this appendix we shall derive equations (2.10a, b) explicitly. They have first been derived for the isotropic case by Majumdar[8]), who did not investigate them any further. However, a concise derivation for general σ seems justified in order to establish our notation and discuss symmetries and suitable reductions of some of the quantities that occur in the equations.

I.1 *Two-magnon T-matrix in the three-magnon subspace*

We first rewrite the energy of three free magnons, eq. (2.5),

$$E(\boldsymbol{k}_1, \boldsymbol{k}_2, \boldsymbol{k}_3) = J \sum_{i=1}^{3} \sum_{d=x,y} (1 - \sigma \cos k_{id})$$

$$= 6J - \sigma J \sum_{d=x,y} (\cos (P_d - K_{md}) + 2 \cos (K_{md}/2) \cos p_{md})$$

$$\equiv E(\boldsymbol{P}, \boldsymbol{K}_m, \boldsymbol{p}_m)$$

with $m = 1, 2, 3$; $\boldsymbol{P}, \boldsymbol{K}_m, \boldsymbol{p}_m$ defined below eq. (2.6). According to eq. (2.6) the matrix elements of the interaction have the structure

$$\langle \boldsymbol{k}_1 \boldsymbol{k}_2 \boldsymbol{k}_3 | \, V | \alpha \rangle = \sum_{j=1}^{3} \sum_{d=x,y} {}_j\langle \boldsymbol{P} \boldsymbol{K}_j \boldsymbol{p}_j | \, V_j^d \, | \alpha \rangle$$

with

$${}_j\langle \boldsymbol{P} \boldsymbol{K}_j \boldsymbol{p}_j | \, V_j^d \, | \alpha \rangle = -(4J/N) \, \delta_{\boldsymbol{P}, \bar{\boldsymbol{P}}} \cos p_{jd}$$

$$\times \sum_{i=1}^{3} \delta_{\boldsymbol{K}_j, \bar{\boldsymbol{K}}_i} (\cos \bar{p}_{id} - \sigma \cos (\bar{K}_{id}/2)). \tag{I.1}$$

$|\alpha\rangle \equiv |\boldsymbol{k}_1, \boldsymbol{k}_2, \boldsymbol{k}_3\rangle$ totally symmetric state defined by (2.4) and $|\boldsymbol{P} \boldsymbol{K}_j \boldsymbol{p}_j\rangle_j$ the state symmetric in all magnons but one (labeled j):

$${}_j\langle \boldsymbol{P} \boldsymbol{K}_j \boldsymbol{p}_j \, | \, \boldsymbol{P}' \boldsymbol{K}_j' \boldsymbol{p}_j' \rangle_j = \delta_{\boldsymbol{P}, \boldsymbol{P}'} \delta_{\boldsymbol{K}_j, \boldsymbol{K}_j'} (\delta_{\boldsymbol{p}_j, \boldsymbol{p}_j'} + \delta_{\boldsymbol{p}_j, -\boldsymbol{p}_j'}).$$

The closure relation for these states has the form

$$\tfrac{1}{2} \sum_{\boldsymbol{P} \boldsymbol{K}_j \boldsymbol{p}_j} |\boldsymbol{P} \boldsymbol{K}_j \boldsymbol{p}_j\rangle_j \, {}_j\langle \boldsymbol{P} \boldsymbol{K}_j \boldsymbol{p}_j | = 1.$$

In the following conservation of total momentum in all matrix elements is understood and $\boldsymbol{P}$ is not explicitly denoted in the states. With the above definitions the Lippmann Schwinger equation for the two-magnon T-matrix can simply be derived. We may write

$${}_j\langle \boldsymbol{K}_j \boldsymbol{p}_j | \, T_j \, | \alpha \rangle = \sum_{d=x,y} {}_j\langle \boldsymbol{K}_j \boldsymbol{p}_j | \, T_j^d \, | \alpha \rangle,$$

where

$${}_1\langle \boldsymbol{K}_1 \boldsymbol{p}_1 | \, T_1^d(E) \, | \alpha \rangle = {}_1\langle \boldsymbol{K}_1 \boldsymbol{p}_1 | \, V_1^d \, | \alpha \rangle$$

$$+ \tfrac{1}{2} \sum_{\boldsymbol{K}_1' \boldsymbol{p}_1'} {}_1\langle \boldsymbol{K}_1 \boldsymbol{p}_1 | \, V_1^d \, | \boldsymbol{K}_1' \boldsymbol{p}_1' \rangle_1 \frac{\Sigma_{d'} \, {}_1\langle \boldsymbol{K}_1' \boldsymbol{p}_1' | \, T_1^{d'} \, | \alpha \rangle}{E - E(\boldsymbol{K}_1', \boldsymbol{p}_1')}$$

$$(d = x, y), \tag{I.2}$$

and completely similar equations hold for ${}_2\langle T_2^d\rangle$ and ${}_3\langle T_3^d\rangle$. We substitute (I.1) into (I.2). Because of the separability of ${}_1\langle V_1^d\rangle$ we have as general solution of (I.2)

$$\langle T_1^d\rangle = \cos p_{1d} U_1^d(\boldsymbol{K}_1, E; \alpha)$$

where U_1^d obeys

$$U_1^d(\boldsymbol{K}_1, E; \alpha) = -\frac{4J}{N}\sum_i \left(\cos \bar{p}_{id} - \sigma \cos\frac{\bar{K}_{id}}{2}\right)\delta_{\bar{K}_i, K_1} - \frac{2J}{N}\sum_{p_1'}\sum_{d'=x,y}\left(\cos p'_{1d} - \sigma\cos\frac{K_{1d}}{2}\right)\frac{\cos p'_{1d'} U_1^{d'}(\boldsymbol{K}_1, E; \alpha)}{E - E(\boldsymbol{K}_1, \boldsymbol{p}_1')} \quad (d = x, y). \tag{I.2a}$$

The algebraic equations for U_1^x and U_1^y can easily be solved. In the thermodynamic limit we may replace

$$-\frac{2J}{N}\sum_{p_1'} \quad \text{by} \quad -\frac{J}{2\pi^2}\int_{-\pi}^{+\pi}\int \mathrm{d}p'_{1x}\,\mathrm{d}p'_{1y}.$$

In this limit the solution of eq. (I.2a) is given by

$$\begin{bmatrix} U_1^x(\boldsymbol{K}_1, E; \alpha) \\ U_1^y(\boldsymbol{K}_1, E; \alpha)\end{bmatrix} = \begin{bmatrix} c_{xx}(t, \beta_x, \beta_y) & c_{xy}(t, \beta_x, \beta_y) \\ c_{yx}(t, \beta_x, \beta_y) & c_{yy}(t, \beta_x, \beta_y)\end{bmatrix}\begin{bmatrix} A_x \\ A_y\end{bmatrix}.$$

Here we have introduced the following expressions

$$A_d = -\frac{4J}{N}\sum_{i=1}^{3}\left(\cos\bar{p}_{id} - \cos\frac{\bar{K}_{id}}{2}\right)\delta_{\bar{K}_i, K_1} \qquad (d = x, y),$$

$$D_1^i(t, \beta_x, \beta_y) = \frac{1}{\pi^2}\int_0^{\pi}\int \mathrm{d}p_x\,\mathrm{d}p_y\,\frac{\cos p_i}{t - \beta_x\cos p_x - \beta_y\cos p_y} \qquad (i = x, y), \tag{I.3a}$$

$$D_2^{ii}(t, \beta_x, \beta_y) = \frac{1}{\pi^2}\int_0^{\pi}\int \mathrm{d}p_x\,\mathrm{d}p_y\,\frac{\cos^2 p_i}{t - \beta_x\cos p_x - \beta_y\cos p_y} \qquad (i = x, y), \tag{I.3b}$$

$$D_2^{ij}(t, \beta_x, \beta_y) = \frac{1}{\pi^2}\int_0^{\pi}\int \mathrm{d}p_x\,\mathrm{d}p_y\,\frac{\cos p_i\cos p_j}{t - \beta_x\cos p_x - \beta_y\cos p_y} \qquad \begin{pmatrix} i, j = x, y \\ i \neq j\end{pmatrix}. \tag{I.3c}$$

$$\mathrm{Det}\,(t, \beta_x, \beta_y) = 1 - D_2^{xx} - D_2^{yy} + \beta_x D_1^x (1 - D_2^{yy}) + \beta_y D_1^y (1 - D_2^{xx}) + (\beta_x D_1^y + \beta_y D_1^x) D_2^{xy} + D_2^{xx} D_2^{yy} - (D_2^{xy})^2. \tag{I.4}$$

$$c_{xx}(t, \beta_x, \beta_y) = (1 - D_2^{yy} + \beta_y D_1^y)/\mathrm{Det}, \tag{I.5a}$$

$$c_{yy}(t, \beta_x, \beta_y) = (1 - D_2^{xx} + \beta_x D_1^x)/\mathrm{Det}, \tag{I.5b}$$

$$c_{xy}(t, \beta_x, \beta_y) = (D_2^{xy} - \beta_x D_1^y)/\mathrm{Det}, \tag{I.5c}$$

$$c_{yx}(t, \beta_x, \beta_y) = (D_2^{yx} - \beta_y D_1^x)/\mathrm{Det}. \tag{I.5d}$$

All omitted arguments on the right-hand side of eqs. (I.4)–(I.5a–d) occur in the order β_x, β_y. Furthermore, in the above equations we have defined

$$t = 3 - E/2J - \tfrac{1}{2}\sigma(\cos(P_x - K_{1x}) + \cos(P_y - K_{1y})),$$

$$\beta_x = \sigma \cos K_{1x}/2, \qquad \beta_y = \sigma \cos K_{1y}/2,$$

so that

$$E - E(\boldsymbol{K}_1, \boldsymbol{p}_1') = -2J(t - \beta_x \cos p_{1x}' - \beta_y \cos p_{1y}').$$

Then for ${}_1\langle \boldsymbol{K}_1 \boldsymbol{p}_1 | T_1 | \alpha \rangle = \sum_{d=x,y} {}_1\langle \boldsymbol{K}_1 \boldsymbol{p}_1 | T_1^d | \alpha \rangle$ we find

$${}_1\langle \boldsymbol{K}_1 \boldsymbol{p}_1 | T_1 | \alpha \rangle = -\frac{4J}{N} \sum_{i=1}^{3} \delta_{\bar{K}_i, K_1} \sum_{\mu, \nu = x, y} c_{\mu\nu}(t, \beta_x, \beta_y) \times \cos p_{1\mu} \left(\cos \bar{p}_{i\nu} - \sigma \cos \frac{\bar{K}_{i\nu}}{2} \right). \tag{I.6}$$

I.2. *The three-magnon T-matrix*

I.2.1. *Faddeev equation for the three-magnon T-matrix*

Following Faddeev the three-magnon T-matrix may be split into three parts: $T = \sum_{i=1}^{3} T^{(i)}$, and the T-matrix elements between totally symmetric states read

$$\langle \boldsymbol{k}_1 \boldsymbol{k}_2 \boldsymbol{k}_3 | T | \alpha \rangle = \sum_{j=1}^{3} \sum_{d=x,y} {}_j\langle \boldsymbol{P} \boldsymbol{K}_j \boldsymbol{p}_j | T_d^{(j)} | \alpha \rangle. \tag{I.7}$$

Writing the Faddeev equations for two of the terms, say ${}_1\langle \boldsymbol{K}_1 \boldsymbol{p}_1 | \, T_d^{(1)} \, | \alpha \rangle$ with $d = x, y$, we have

$$
\begin{aligned}
{}_1\langle \boldsymbol{K}_1 \boldsymbol{p}_1 | \, T_d^{(1)} \, | \alpha \rangle = {}& {}_1\langle \boldsymbol{K}_1 \boldsymbol{p}_1 | \, T_1^d \, | \alpha \rangle \\
& + \tfrac{1}{2} \sum_{\boldsymbol{K}_2' \boldsymbol{p}_2'} {}_1\langle \boldsymbol{K}_1 \boldsymbol{p}_1 | \, T_1^d \, | \boldsymbol{K}_2' \boldsymbol{p}_2' \rangle_2 \, \frac{\sum_{d'=x,y} {}_2\langle \boldsymbol{K}_2' \boldsymbol{p}_2' | \, T_{d'}^{(2)} \, | \alpha \rangle}{E - E(\boldsymbol{K}_2', \boldsymbol{p}_2')} \\
& + \tfrac{1}{2} \sum_{\boldsymbol{K}_3', \boldsymbol{p}_3'} {}_1\langle \boldsymbol{K}_1 \boldsymbol{p}_1 | \, T_1^d \, | \boldsymbol{K}_3' \boldsymbol{p}_3' \rangle_3 \, \frac{\sum_{d'=x,y} {}_3\langle \boldsymbol{K}_3' \boldsymbol{p}_3' | \, T_{d'}^{(3)} \, | \alpha \rangle}{E - E(\boldsymbol{K}_3', \boldsymbol{p}_3')} \\
& (d = x, y), \qquad \text{(I.8)}
\end{aligned}
$$

where ${}_1\langle T_1^d \rangle_m$ are two-magnon T-matrix elements. We may now substitute the result (I.6) of the two-magnon T-matrix, which is separable just like the interaction. Hence the general solution for ${}_1\langle T_d^{(1)} \rangle$ reads

$${}_1\langle \boldsymbol{K}_1 \boldsymbol{p}_1 | \, T_d^{(1)} \, | \alpha \rangle = \cos p_{1d} \varphi_d^{(1)}(\boldsymbol{K}_1, E; \alpha) \qquad (d = x, y).$$

The equations for $T_d^{(2)}$ and $T_d^{(3)}$ are entirely similar to (I.8), and the same argument can be made. Therefore, we have in general ($d = x, y$):

$${}_j\langle \boldsymbol{K}_j \boldsymbol{p}_j | \, T_d^{(j)} \, | \alpha \rangle = \cos p_{jd} \varphi_d^{(j)}(\boldsymbol{K}_j, E; \alpha) \qquad (j = 1, 2, 3). \qquad \text{(I.9)}$$

Since $\langle \boldsymbol{k}_1 \boldsymbol{k}_2 \boldsymbol{k}_3 | \, T \, | \alpha \rangle$ is invariant under the exchange of any two magnons, we may infer from (I.7) that all functions $\varphi_d^{(j)}$ for $j = 1, 2, 3$ are the same functions of their arguments $\boldsymbol{K}_j$. Now, using the following identities

$$|\boldsymbol{K}_2 \boldsymbol{p}_2\rangle_2 = |\boldsymbol{K}_1^{(2)} \boldsymbol{p}_1^{(2)}\rangle_1 = |\boldsymbol{P} - \tfrac{1}{2}\boldsymbol{K}_2 + \boldsymbol{p}_2, \tfrac{1}{2}\boldsymbol{P} - \tfrac{3}{4}\boldsymbol{K}_2 - \tfrac{1}{2}\boldsymbol{p}_2\rangle_1, \qquad \text{(I.10a)}$$

$$|\boldsymbol{K}_3 \boldsymbol{p}_3\rangle_3 = |\boldsymbol{K}_1^{(3)} \boldsymbol{p}_1^{(3)}\rangle_1 = |\boldsymbol{P} - \tfrac{1}{2}\boldsymbol{K}_3 - \boldsymbol{p}_3, -\tfrac{1}{2}\boldsymbol{P} + \tfrac{3}{4}\boldsymbol{K}_3 - \tfrac{1}{2}\boldsymbol{p}_3\rangle_1 \qquad \text{(I.10b)}$$

and dropping all irrelevant subscripts on the momentum variables, we arrive at the following equations for φ_x and φ_y

$$
\begin{aligned}
& \varphi_d(\boldsymbol{K}, E; \alpha) \\
& = -\frac{4J}{N} \sum_{j=1}^{3} \delta_{\bar{K}_j, K} \sum_{v=x,y} c_{dv}(t, \beta_x, \beta_y) \left(\cos \bar{p}_{jv} - \sigma \cos \frac{\bar{K}_{jv}}{2} \right) \\
& \quad + \frac{2}{N} \sum_{K'} \sum_{v=x,y} c_{dv}(t, \beta_x, \beta_y) \\
& \quad \times \frac{[\cos(P_v - K_v' - \tfrac{1}{2}K_v) - \sigma \cos K_v/2]}{(t - \beta_x \cos(P_x - K_x' - \tfrac{1}{2}K_x) - \beta_y \cos(P_y - K_y' - \tfrac{1}{2}K_y))} \\
& \quad \times \sum_{d'=x,y} \cos(K_{d'} - P_{d'} + \tfrac{1}{2}K_{d'}') \, \varphi_{d'}(K', E; \alpha) \qquad \text{(I.11)}
\end{aligned}
$$

with $t = 3 - \frac{1}{2}E - \frac{1}{2}\sigma(\cos(P_x - K_x) + \cos(P_y - K_y))$ and $\beta_\nu = \sigma \cos K_\nu/2$ $(\nu = x, y)$.

For values of E in the neighbourhood of a bound state energy the inhomogeneous term may be omitted, and taking $\lim N \to \infty$ we obtain eqs. (2.10a, b) for φ_x and φ_y.

I.2.2. *The functions* D_1^ν *and* $D_2^{\mu\nu}$

The quantities defined by (I.3) are the same as introduced by Wortis[4]). They obey the following relations

$$D_1^\nu(t, \beta_x, \beta_y) = D_1^{\bar{\nu}}(t, \beta_y, \beta_x) \qquad (\nu = x, y), \tag{I.12a}$$

$$D_2^{\mu\nu}(t, \beta_x, \beta_y) = D_2^{\bar{\mu}\bar{\nu}}(t, \beta_y, \beta_x) \qquad (\mu, \nu = x, y), \tag{I.12b}$$

$$D_2^{\mu\nu}(t, \beta_x, \beta_y) = D_2^{\nu\mu}(t, \beta_x, \beta_y) \qquad (\mu \neq \nu), \tag{I.12c}$$

where $\bar{\nu} = x(y)$ if $\nu = y(x)$, *etc.*

From these relations the properties (2.6) of c_{ij} follow. D_1^ν and $D_2^{\mu\nu}$ may be expresses in terms of elliptic integrals, but we calculate them numerically in the following manner. In $D_1^x(t, \beta_x, \beta_y)$ one integration may be done analytically. One obtains

$$D_1^x(t, \beta_x, \beta_y) \equiv \frac{1}{\pi^2} \int_0^\pi\int_0^\pi \mathrm{d}p_x\, \mathrm{d}p_y \frac{\cos p_x}{t - \beta_x \cos p_x - \beta_y \cos p_y}$$

$$= \frac{1}{\pi} \int_0^\pi \mathrm{d}p_x \frac{\cos p_x}{[(t - \beta_x \cos p_x)^2 - \beta_y^2]^{\frac{1}{2}}} \qquad \text{if} \quad t \geqslant \beta_x + \beta_y \geqslant 0,$$

which condition is fulfilled for all values of E below the three-magnon band. Similarly

$$D_2^{xx}(t, \beta_x, \beta_y) = \frac{1}{\pi} \int_0^\pi \mathrm{d}p_x \frac{\cos^2 p_x}{[(t - \beta_x \cos p_x)^2 - \beta_y^2]^{\frac{1}{2}}}.$$

These two integrals are calculated numerically. D_1^y and D_2^{yy} are obtained by using (I.12a) and (I.12b), D_2^{xy} is found from the relation:

$$tD_1^x(t, \beta_x, \beta_y) = \beta_x D_2^{xx}(t, \beta_x, \beta_y) + \beta_y D_2^{xy}(t, \beta_x, \beta_y).$$

Appendix II

In this appendix it is indicated how the bottom of the band of three-magnon states, appearing in the figures, is obtained. The bottom of the band of scattering states of three free magnons may easily be found analytically by minimizing the expression for the energy

$$E(\boldsymbol{k}_1, \boldsymbol{k}_2, \boldsymbol{k}_3) = \sum_{i=1}^{3} \sum_{d=x,y} (1 - \sigma \cos k_{id})$$

with respect to the variables k_{id}, subject to the condition that $\boldsymbol{k}_1 + \boldsymbol{k}_2 + \boldsymbol{k}_3 = \boldsymbol{P}$, and that all momenta $\boldsymbol{k}_i$ are confined to the first Brillouin zone. Thus one finds for the bottom of this band at given $\boldsymbol{P}$

$$E^{(3)}(P_x, P_y; \sigma) = 6 - 3\sigma(\cos \tfrac{1}{3}P_x + \cos \tfrac{1}{3}P_y) \tag{II.1}$$

and this minimum is reached at $k_{1i} = k_{2i} = k_{3i} = P_i/3$ $(i = x, y)$.

The bottom of a band of states in which one magnon of energy $2 - \sigma \cos k_x - \sigma \cos k_y$ is scattered by a two-magnon bound state of energy E_B, has to be determined numerically since no analytic expression can be obtained for E_B as a function of $\boldsymbol{K} = (K_x, K_y)$, the total momentum of the two-magnon bound state. There are as many of these bands, as there are different two-magnon bound states energies. The bottom $E^{(2,1)}(P_x, P_y; \sigma; E_B)$ of each is given by

$$E^{(2,1)}(P_x, P_y; \sigma; E_B) = \operatorname*{Min}_{\boldsymbol{K}} [4 - 2t_B(\boldsymbol{K}; \sigma) + (2 - \sigma \cos(P_x - K_x) - \sigma \cos(P_y - K_y))], \tag{II.2}$$

where $t_B(\boldsymbol{K}; \sigma) \equiv 2 - E_B(\boldsymbol{K}, \sigma)/2$. The two-magnon bound state energies are found by solving $t = 2 - E/2$ from the two-magnon bound state condition, obtained by putting (I.4) equal to zero:

$$1 - \sum_{\substack{i,j=x,y \\ i \neq j}} (D_2^{ii} - \beta_i D_1^i + \beta_i D_1^i D_2^{jj} - \beta_i D_1^j D_2^{ij} - \tfrac{1}{2} D_2^{ii} D_2^{jj} + \tfrac{1}{2}(D_2^{ij})^2) = 0, \tag{II.3}$$

where all D-functions depend on $\beta_x = \sigma \cos K_x/2$, $\beta_y = \sigma \cos K_y/2$ and t. Now we know[4]), that there are two two-magnon bound states. One, at energy $E_B^{(1)}$, exists for all values of $\boldsymbol{K}$; the other, at energy $E_B^{(2)}$, only at small enough values of β_i, but whenever it exists $E_B^{(2)} \geqslant E_B^{(1)}$. Hence $E^{(2,1)}(P_x, P_y; \sigma; E_B^{(1)}) \leqslant E^{(2,1)}(P_x, P_y; \sigma; E_B^{(2)})$. In view of this and the fact, that $E^{(2,1)}(P_x, P_y; \sigma; E_B^{(1)}) < E^{(3)}(P_x, P_y; \sigma)$, the bottom of the band which is shown in the figures, is simply given by $E^{(2,1)}(P_x, P_y; \sigma; E_B^{(1)})$. In the case of fig. 3 the minimum (II.2) is reached at $\beta_x = \beta_y = \beta$, where, as one sees easily, β satisfies the equation $\mathrm{d}t/\mathrm{d}\beta = (4/\sigma)\beta$.

From fig. 10 it is evident that $\beta = 0$ is the only solution to this equation provided $\sigma < 0.8$. Hence, for $\sigma < 0.8$, $E^{(2,1)}(\pi, \pi; \sigma; E_B^{(1)}) = 5 - 2\sigma$, so the bottom of the band is given by a straight line.

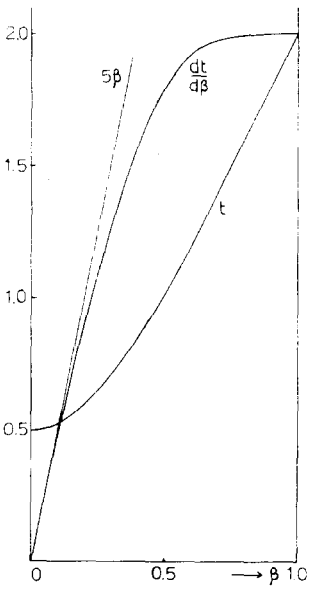

Fig. 10. $t = 2 - E_B^{(1)}/2$ and $dt/d\beta$ as a function of β for the case $\beta_x = \beta_y = \beta$.

References

1) J.B.Torrance and M.Tinkham, Phys. Rev. **187** (1969) 587.
2) J.B.Torrance and M.Tinkham, Phys. Rev. **187** (1969) 595.
3) F.J.Dyson, Phys. Rev. **102** (1956) 1217.
4) M.Wortis, Phys. Rev. **132** (1963) 85.
5) J.G.Hanus, Phys. Rev. Letters **11** (1963) 336.
6) H.A.Bethe, Z. Physik **71** (1931) 205.
7) I.G.Gochev, Sov. Phys. JETP **34** (1972) 892.
8) C.K.Majumdar, Phys. Rev. **B1** (1970) 287.
9) C.K.Majumdar and G.Mukhopadhyay, Phys. Letters **31A** (1970) 321.
10) H.C.Fogedby, Phys. Rev. **B5** (1972) 1941.
11) L.J.de Jongh and A.R.Miedema, Adv. in Physics **23** (1974) 1.
12) J.E.van Himbergen and J.A.Tjon, Physica **76** (1974) 503.
13) N.Fukuda and M.Wortis, J. Phys. Chem. Solids **24** (1963) 1675.
14) L.Faddeev, Sov. Phys. JETP **12** (1961) 1014.
15) S.Maleev, Sov. Phys. JETP **6** (1958) 776.
16) J.E.van Himbergen and J.A.Tjon, Phys. Letters **50A** (1974) 189.

17) J.S.R.Chisholm, in Padé Approximants, P.R.Graves-Morris, ed. (The Institute of Physics, London and Bristol, 1972).
18) J.A.Tjon, in Padé Approximants and their Applications, P.R.Graves-Morris, ed. (Academic Press, New York, 1973).
19) D.I.Lalović *et al.*, Nuovo Cim. **68B** (1970) 75.
20) R.G.Boyd and J.Callaway, Phys. Rev. **138** (1965) 1621.
21) L.R.Dodd, J. Math. Phys. **11** (1970) **207**.
22) C.K.Majumdar, J. Math. Phys. **13** (1972) 705.
23) R.Silberglitt and A.Brooks Harris, Phys. Rev. **174** (1968) 640.
24) R.Silberglitt, Phys. Rev. **188** (1969) 786.
25) H.Kinder, Phys. Rev. Letters **28** (1972) 1564.
26) I.G.Gochev, Phys. Letters **53A** (1975) 195.